

Article

A Multi-Scale Virtual Terrain for Hierarchically Structured Non-Location Data

Rui Xin ¹, Tinghua Ai ^{2,*} , Ruoxin Zhu ³ , Bo Ai ¹, Min Yang ² and Liqiu Meng ⁴

¹ College of Geodesy and Geomatics, Shandong University of Science and Technology, Qingdao 266590, China; xinrui@sdust.edu.cn (R.X.); aibo@sdust.edu.cn (B.A.)

² School of Resource and Environment Sciences, Wuhan University, Wuhan 430072, China; yangmin2003@whu.edu.cn

³ State Key Laboratory of Geo-Information Engineering, Xi'an Research Institute of Surveying and Mapping, Xi'an 710054, China; ruoxin.zhu@tum.de

⁴ Chair of Cartography, Technical University of Munich, 80333 München, Germany; liqiu.meng@tum.de

* Correspondence: tinghuaai@whu.edu.cn; Tel.: +86-139-0863-9199

Abstract: Metaphor are commonly used rhetorical devices in linguistics. Among the various types, spatial metaphors are relatively common because of their intuitive and sensible nature. There are also many studies that use spatial metaphors to express non-location data in the field of visualization. For instance, some virtual terrains can be built based on computer technologies and visualization methods. In virtual terrains, the original abstract data can obtain specific positions, shapes, colors, etc. and people's visual and image thinking can play a role. In addition, the theories and methods used in the space field could be applied to help people observe and analyze abstract data. However, current research has limited the use of these space theories and methods. For instance, many existing map theories and methods are not well combined. In addition, it is difficult to fully display data in virtual terrains, such as showing the structure and relationship at the same time. Facing the above problems, this study takes hierarchical data as the research object and expresses both the data structure and relationship from a spatial perspective. First, the conversion from high-dimensional non-location data to two-dimensional discrete points is achieved by a dimensionality reduction algorithm to reflect the data relationship. Based on this, kernel density estimation interpolation and fractal noise algorithms are used to construct terrain features in the virtual terrains. Under the control of the kernel density search radius and noise proportion, a multi-scale terrain model is built with the help of level of detail (LOD) technology to express the hierarchical structure and support the multi-scale analysis of data. Finally, experiments with actual data are carried out to verify the proposed method.

Keywords: virtual terrain; map-like visualization; map metaphor; non-location hierarchical data; multi-scale representation



Citation: Xin, R.; Ai, T.; Zhu, R.; Ai, B.; Yang, M.; Meng, L. A Multi-Scale Virtual Terrain for Hierarchically Structured Non-Location Data. *ISPRS Int. J. Geo-Inf.* **2021**, *10*, 379. <https://doi.org/10.3390/ijgi10060379>

Academic Editor: Wolfgang Kainz

Received: 4 April 2021

Accepted: 26 May 2021

Published: 3 June 2021

Publisher's Note: MDPI stays neutral with regard to jurisdictional claims in published maps and institutional affiliations.



Copyright: © 2021 by the authors. Licensee MDPI, Basel, Switzerland. This article is an open access article distributed under the terms and conditions of the Creative Commons Attribution (CC BY) license (<https://creativecommons.org/licenses/by/4.0/>).

1. Introduction

In the past few decades, our living environment has undergone tremendous changes. The real physical environment is flanked by many virtual environments. With the nearly ubiquitously accessible Internet and telecommunication devices, people spend an increasing amount of time interacting with a digital information space in contrast to the traditional visible and tangible physical space.

The aforementioned extension in the meaning of traditional space brings about the following changes: (1) The concept of spatial objects now includes not only geospatial objects but also objects in information space. (2) The nature of spatial objects has changed. Geospatial objects usually have attributes such as shape, size and weight, which can be directly perceived by sight, touch, etc. In particular, these objects have location information, and their positions can be determined by coordinates. The objects in information space also have a series of attributes; however, these attributes are not intuitive, often requiring the

observer to read and think logically before recognition. They usually have no coordinates and cannot be located. In addition, they mostly have hidden structures and relationships. All these differences necessitate the extension of spatial descriptions to accommodate the non-location data in the information space.

The term spatialization is used to describe the process from handling to rendering of non-location data with map metaphors because maps are the most widespread tools for spatial description [1]. Maps adapted to the changed meanings of space as container of non-location data are called map-like visualizations [2]. The rise of map-like visualizations in the context of spatialization may considerably broaden the scope of conventional maps, enrich the associated cartographic theories and extend the applications beyond the geospatial domain.

The current map-like visualizations take either polygons or virtual terrains as the information carriers. The former often simulates the administrative map in the form of polygon nesting [3,4]. The latter simulates natural landforms using landscape metaphors [5]. This study focuses mainly on the latter. In virtual terrain map-like visualizations, the height metaphor is used to reflect numerical attribute values, whereas the distance is a suitable metaphor for similarity and relevance [6]. However, hidden structures, such as hierarchical structures, are often difficult to reflect in virtual terrains, although multi-scale ideas are highly valued in relevant theoretical research in map-like visualization [7].

This study aims to design a map-like visualization that is able to display the contents, relationships and structures of non-location data. Compared with other types of map-like visualization studies that focus on showing only the single-dimensional features of data, this study shows the data features more comprehensively through the migration application and mutual integration of various methods in visualization and geographic information system (GIS). This provides a feasible technical scheme for the terrain multi-scale expression and visual analysis of non-spatial hierarchical data. For hierarchical data, a virtual terrain is constructed to visualize both the hierarchical structure and relationships among data items. The multi-scale idea is introduced into virtual terrain with the help of level of detail (LOD) technology [8]. A multi-scale representation model that combines scales in maps with the hierarchy in data is built. Virtual terrains with different levels of detail are constructed by using kernel density estimation interpolation and fractal noise. With the help of virtual terrain, multi-scale visual expression and analysis can be carried out. The rest of the paper is organized as follows. Section 2 introduces related works. Section 3 is dedicated to specific methods. The experiments and analysis are presented in Section 4, which is followed by concluding remarks in Section 5.

2. Related Works

Spatialization has been addressed by different researchers but from similar perspectives. According to Fabrikant et al. spatialization is the design of spatial graphics for non-location data whose content and structure are described by means of spatial metaphors [5]. Skupin and Buttenfield defined spatialization in information space as “a projection of elements of a high-dimensional information space into a low-dimensional, potentially experiential, representational space” [9].

Spatialization has also been explored in cognitive experiments. For instance, spatial metaphors were inspected in various displays of spatialization, including point-display [10], network-display [11] and region-display [12], and spatial distance was studied as a metaphor for the relative similarity. Montello et al. [10] proposed the first law of cognitive geography based on the influence of distance on similarity discrimination. Compared with the classical first law of geography [13], the first law of cognitive geography is applied the other way around. It is usually the similarity between objects that determines their distance apart and locations [14].

Researchers have built many map-like visualization works around spatialization [15]. Administrative maps with polygons as map units are a common map form in daily life. In recent years, non-spatial multi-source data expressed in the form of administrative

maps have received attention in the field of visualization [16,17]. Many data visualization explorations have also been carried out based on this kind of map [18]. Terrain maps are another important form of map expression as shown in Table 1. Research on using virtual terrain to express non-spatial data is not sufficient at present. In the field of traditional map visualization, the distribution of spatial statistical data can be described using a landscape metaphor [19,20]. In terms of map-like visualizations, Chalmers explained the rationality of spatialization in terms of cognitive familiarity when landscape metaphors were used for the visualization and search of the corpus [21]. “ThemeScapes” was designed to present text items in a virtual terrain with terrain features, such as mountain peaks and valleys, allowing users to navigate through information space [22,23]. “VxInsight” was another example developed by Boyack et al. with the main purpose of conducting analysis related to the management of science and technology [24].

Table 1. Summary table of typical virtual terrain map-like visualization studies.

Reference	Research Type	Application Domain	Main Work
Using a landscape metaphor to represent a corpus of documents	Method design	Search and retrieval of documents	It builds and displays document corpus in the form of a map constructed from the patterns of similarity and dissimilarity.
Visualizing the non-visual: Spatial analysis and interaction with information from text documents	Method design	Visualization of digital libraries, regulations and procedures, archived reports, etc.	It constructs landscape visualization of text to enhance visual browsing and analysis.
The ecological approach to text visualization	Theoretical research and method design	Science of text visualization	It images information from text documents as natural terrains that are in line with human cognitive predilections.
Domain visualization using VxInsight® for science and technology management	Method design	Science and technology management	It presents the application of a knowledge visualization tool VxInsight® to enable domain analysis for science and technology management within the enterprise.
GraphSplatting: Visualizing graphs as continuous fields	Method design	Map representation of graphs	It introduces a technique that transforms a graph into a two-dimensional scalar field.
Drawing clustered graphs as topographic maps	Method design	Map representation of graphs	It introduces a method that converts clustered graphs into topographic maps.

The basic process of virtual terrain visualization starts with the transformation of abstract data into a virtual space following the first law of cognitive geography. The characteristics of spatial objects in the virtual space may represent the attributes, while spatial relationships such as the distance and clustering are used to express the similarity relation or relevance. Furthermore, data structures can also be reflected in map-like visualizations. For instance, a nested polygon structure can be used to represent hierarchical data [25]. Some earlier studies of virtual terrain for the presentation of data structures mainly focused on the graph structure that reflects the relevance relation. Van and Destudied published papers by constructing a graph structure and transforming the graph into a continuous two-dimensional field [26]. There are also studies in which graph structures are superimposed on virtual terrain to obtain a more obvious display of the data structure [27]. However, compared with the graph structure, the extension of the hierarchy structure is

more diverse. Generally, the graph structure has only horizontal extensions, while the hierarchical structure has an additional level of depth. In the studies on virtual terrains thus far, there is little presentation of the depth of hierarchical structure, and even fewer studies could be found on the comprehensive presentations covering content, relationship and structure at the same time.

In general, the current research works on virtual terrains have not yet made full use of the expressiveness of maps. According to Skupin, the research of this field should not only imitate the form of the map but also draw lessons from the theories and methods of cartography [28]. Keeping this advice in mind, this study introduces ideas such as map multi-scale representations into virtual terrain and thus adds the depth to allow the visualization and analysis of hierarchical data.

3. Methodology

The framework of this study mainly includes spatialization, terrain processing, multi-scale terrain expression, which involves key methods such as multidimensional scaling (MDS), kernel density estimation interpolation, fractal noise and LOD. Each method is applied in accordance with the sequence to complete the virtual terrain representation of hierarchical non-spatial data. Among them, MDS is responsible for the spatial layout of discrete points of non-spatial data. Kernel density estimation interpolation and fractal noise are used to construct the terrain framework and shape the details, respectively, based on these discrete points. Finally, the multi-scale expression of terrain is realized by the combination of LOD. Please refer to Supplementary Materials for the implementation codes of related methods.

Figure 1 shows the methodological framework. 1. The non-location hierarchical data are spatialized as discrete points on a plane by means of a similarity matrix, the MDS and a hierarchical layout strategy. 2. Kernel density estimation interpolation is introduced to convert discrete points into continuous fields representing virtual terrain. In addition, fractal noise can be used to add surface detail features of the terrain. 3. A multi-scale model is built for hierarchical data with the LOD. Under the joint control of the kernel density search radius and noise proportion, terrain scenes of different scales are output to facilitate multi-scale representation and analysis.

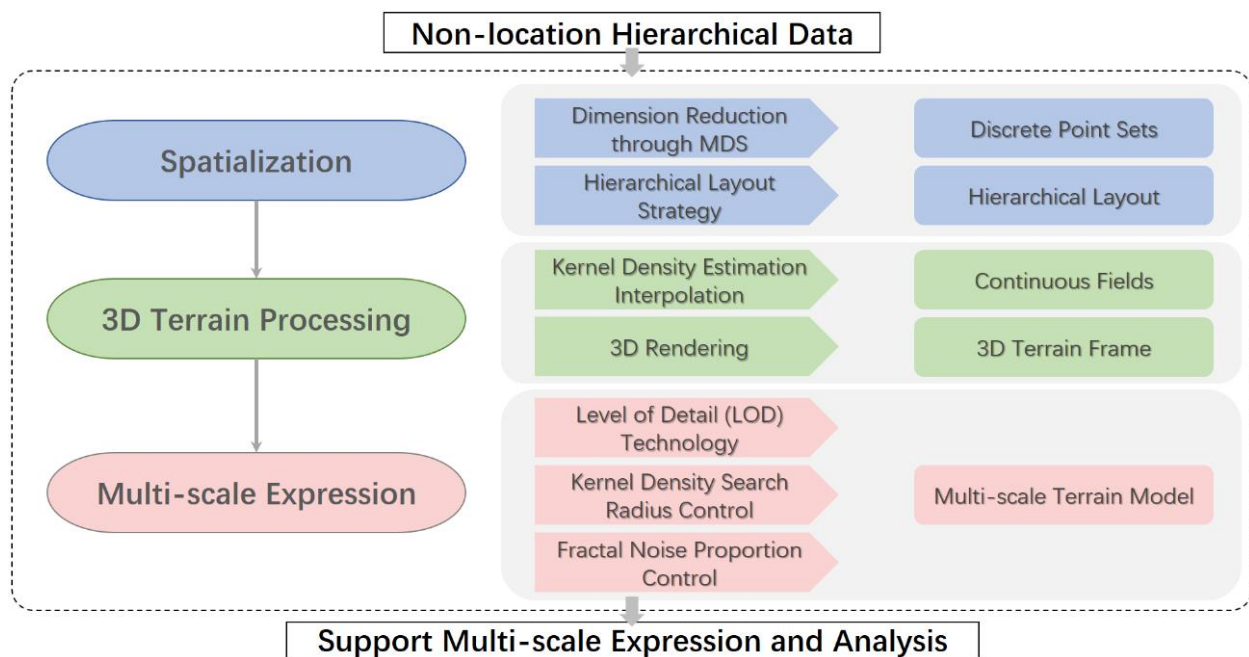


Figure 1. Methodological framework.

3.1. Spatial Layout of Non-Location Data

3.1.1. Dimension Reduction

Data in the information space are mostly high dimensional, abstract and hard to recognize. Generally, these data are mapped onto a low-dimensional space by dimension reduction so that relative positions in space can reflect the data relationship. Among many dimension reduction methods, MDS and self-organizing maps (SOMs) are widely used in spatialization [29]. SOM has the advantage of maintaining the topological relationship of data, whereas MDS is focused on the distance metaphor to reflect data similarity. This study aims to visualize the data similarity and aggregation through dimension reduction. Therefore, MDS is selected.

In the MDS method, n multidimensional data items are taken as contents to be explored, and the similarity relationship between items i and j ($i, j = 1, 2, \dots, n$) can be represented by S_{ij} . A similarity matrix $[S_{ij}]$ is imported to MDS to obtain the spatial positions of the individual data items. These spatial positions can be described using $[X_{nm}]$, in which n is the item count and m is the dimension. In the current research, a two-dimensional spatial layout is selected for easy observation and display. Therefore, a series of discrete points created by MDS can represent the original data items, and the spatial distances between them are used to reflect their similarity.

The details of the algorithm are as follows:

1. The similarity matrix $[S_{ij}]$ is subjected to a powered operation to obtain $P^{(2)}$.
2. $P^{(2)}$ is double centered to obtain the result matrix B . The specific calculation process is shown in Function (1), where the definition of J is shown in Function (2), E is the unit $n \times n$ matrix and I is an $n \times n$ matrix of ones.
3. For matrix B in 2, the maximum m eigenvalues are calculated to form diagonal matrix E , and the corresponding m eigenvectors form matrix F . Finally, the coordinate set of discrete points is $F \times E$.

$$B = -\frac{1}{2}JP^{(2)}J \quad (1)$$

$$J = E - n^{-1} \cdot I \quad (2)$$

3.1.2. Hierarchical Layout Strategy

The use of the MDS method can reflect the similarity between data items, but not the structural features of data. The hierarchical order is implicitly embedded in the data. If all data items without making specific distinctions are input into the MDS, the implicit hierarchy will be destroyed.

In view of the heterogeneity of data at different levels and the homogeneity of data at the same level, this study adopts a hierarchical dimension reduction approach. First, data items at the top hierarchical level are laid out through MDS and determine their locations. Then, the sub-data items of each positioned data item are laid out within its neighborhood. This process continues from the top to the bottom until all leaf nodes in the hierarchical data have been traversed.

The specific implementation process of the abovementioned method is as follows:

4. For the sub-data items of the same parent, input the similarity matrix S into the MDS and obtain the layout result, as shown in Figure 2a.
5. Calculate the distance D between the nearest two points in the plane based on the current layout result. Set the neighborhood range for each data item in step 1 as shown in Figure 2b and obtain the square with the data item point in the center and $2/3D$ as the side length.
6. Calculate the layout for the sub-data items of each data item in step 1 and map the layout results to the neighborhood range of their parent. As Function (3) shows, for sub-data item points, choose the maximum distance between two points in the horizontal and vertical directions and assign it to K . Divide K by the side length

of the neighborhood range, and obtain the proportional coefficient G . Calculate the coordinates of the center point of discrete points by Function (4). As shown in Figure 3, take two center points (the center point of discrete points (X_{lc}, Y_{lc}) and the center point of parent neighborhood range (X_{zc}, Y_{zc})) as reference points and map each discrete point (X_l, Y_l) to the parent neighborhood range through Function (5) to obtain their coordinates (X_z, Y_z) .

- Carry out steps 1, 2 and 3 for each data item of hierarchical data from top to bottom until all leaf data items are completely laid out spatially.

$$\begin{aligned} H &= X_{Max} - X_{Min} \\ V &= Y_{Max} - Y_{Min} \\ K &= \text{Max}\{H, V\} \end{aligned} \tag{3}$$

$$\begin{aligned} X_{lc} &= \frac{X_{Max} + X_{Min}}{2} \\ Y_{lc} &= \frac{Y_{Max} + Y_{Min}}{2} \end{aligned} \tag{4}$$

$$\begin{aligned} X_z &= X_{zc} + \frac{X_l - X_{lc}}{G} \\ Y_z &= Y_{zc} + \frac{Y_l - Y_{lc}}{G} \end{aligned} \tag{5}$$

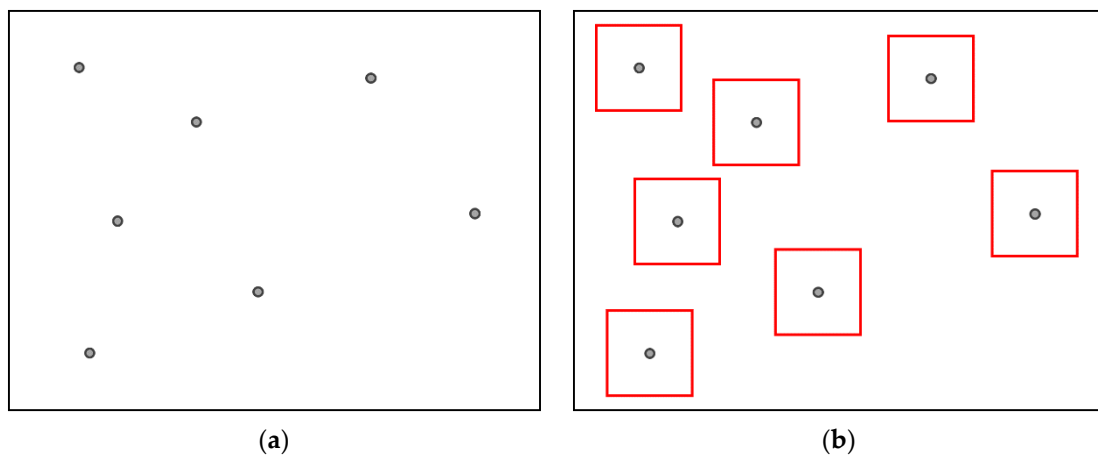


Figure 2. (a) Spatial layout of the data items; (b) neighborhood ranges for the individual data items.

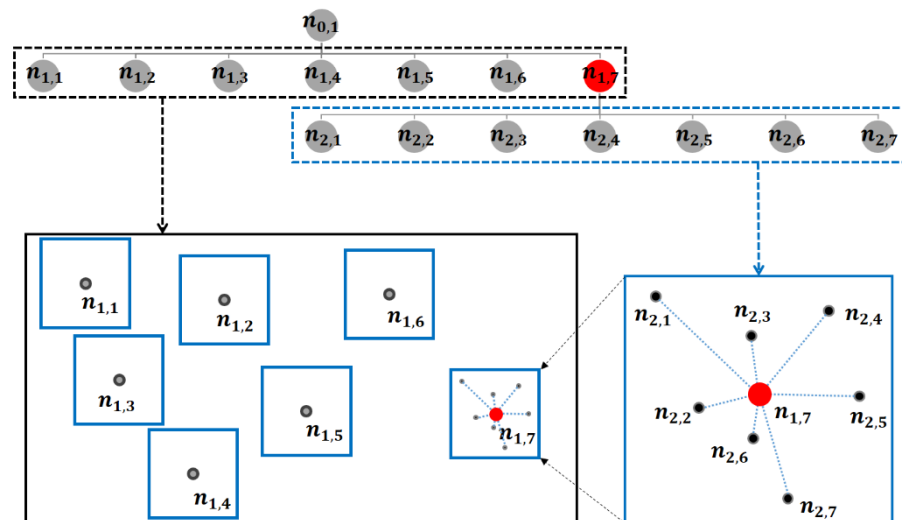


Figure 3. Spatial positioning of sub-nodes in hierarchical data.

3.2. Skeleton Construction of a Virtual Terrain

3.2.1. Field Model Construction Method

The discrete points should be transformed into a continuous field to complete the subsequent construction of a virtual terrain. In this process, spatial interpolation is needed with the aim of modelling the discrete points as a set of high and low undulating mountains. In addition, the relationships of individual data items presented by spatial location, such as aggregation, need to be reflected.

As shown in Figure 4, kernel density estimation interpolation is carried out using the sample data. The interpolation results appear as undulating surfaces, which are similar to the combination of mountain peaks and valleys in the frame structure. More importantly, when carrying out the kernel density estimation, the attributes of multiple objects are accumulated in the spatial neighborhoods. This can reflect the comprehensive influence of each object on the interpolation point, thus expressing the relationship between objects. For instance, places with dense points and high attribute values are often high-value areas, which can be modelled as high-altitude peaks. In addition, kernel density estimation interpolation can control the range of the neighborhood by parameter setting and help investigate data relations at different scales. In view of such characteristics of kernel density estimation interpolation, this study applies this method to the transformation from discrete points to a continuous field.

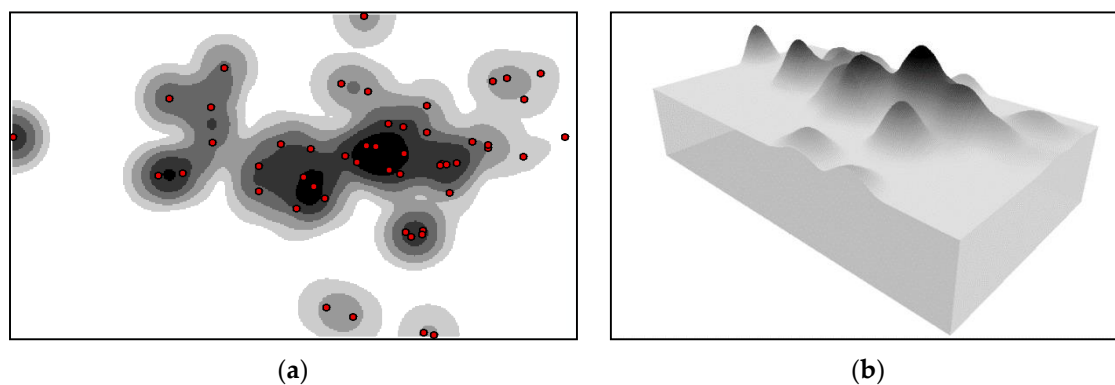


Figure 4. Interpolation results of kernel density estimation interpolation: (a) two-dimensional result; (b) three-dimensional result.

3.2.2. Landform Construction Based on Kernel Density Estimation

In kernel density estimation, each discrete point serves as the core to calculate the estimated values of kernel density around the neighborhood [30]. The function of kernel density estimation is shown in Function (6), in which h is the search radius ($h > 0$), n is the number of discrete points and $K(x)$ is the kernel function. The kernel function in this study is shown in Function (7).

$$f(x) = \frac{1}{nh} \sum_{i=1}^n K \left\{ \frac{1}{h} (x - X_i) \right\} \quad (6)$$

$$K_2(x) = \begin{cases} 3\pi^{-1}(1 - x^T x)^2 & \text{if } x^T x < 1 \\ 0 & \text{otherwise} \end{cases} \quad (7)$$

Different search radii and interpolating attribute values have different effects on the constructed terrain. First, the terrain is constructed by a single point. At this point, the terrain features are mainly related to data features and seldom involve the expression of data relations. Figure 5 presents the top view, front view and oblique view of a mountain affected by different attribute values and search radii. When the attribute value is high and the search radius is small, the mountain form in Figure 5a is constructed, which is thin and tall, as in the case of an isolated peak. When the attribute value is high and the search radius is large, a short and wide mountain form is constructed, as shown in Figure 5b. In a

comparison of the two, the mountain in Figure 5a is steeper and has a higher altitude, the slope of the mountain in Figure 5b is more gradual and the mountain has a larger extension range. When the attribute value is low, the contrast between the corresponding mountains in Figure 5c,d is similar to that in Figure 5a,b. The difference is that the altitudes of the two mountains in Figure 5c,d are lower.

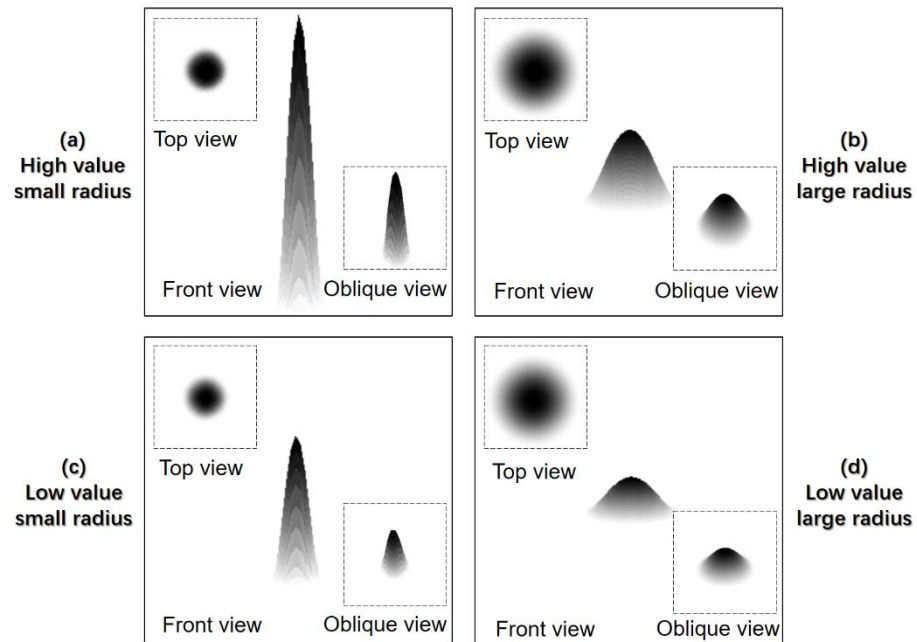


Figure 5. Different perspectives of terrains of different parameters.

As shown in Figure 6, the orthogonal axis is used to generalize the above rule, in which the horizontal axis represents the search radius, and the vertical axis represents the attribute value. The attribute value influences the altitude of the mountain, and there is a positive correlation between them. When the search radius does not change, the increase in the attribute value leads to an increase in the altitude of the mountain. The search radius influences the range of the mountain, and there is a positive correlation between the two parameters. When the attribute value does not change, the range of the mountain increases as the search radius increases.

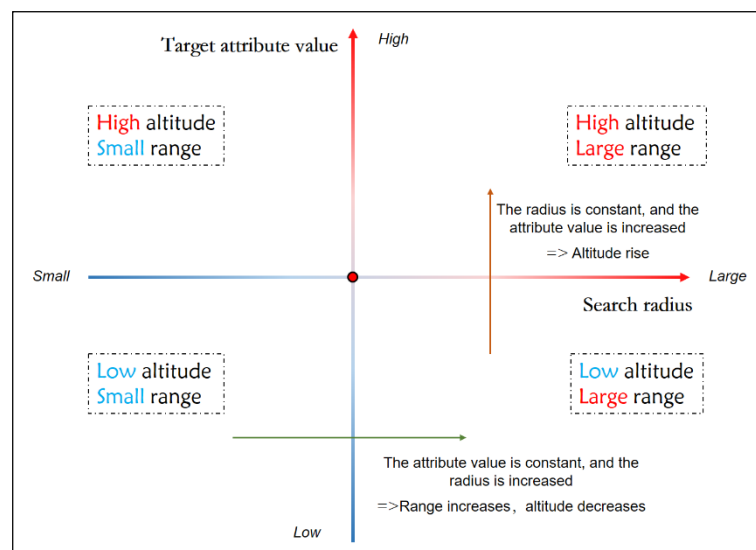


Figure 6. Orthogonal axis description of terrain parameters.

When the terrain is constructed by two or more points, the feature terrain that describes the relationship hidden in the data appears in addition to the terrain that describes the content of the data. First, as shown in Figure 7, two points with the same target attribute value are observed. A small search radius leads to a large gap between the two mountains. This creates a valley form, as shown in Figure 7a. As the search radius increases, the gap between the two mountains is partially filled to realize the connection between the mountains, which also forms terrain characteristics similar to a saddle (see Figure 7b). The increases in search radius result in the continuous filling of the gap between mountains, which leads to the disappearance of the saddle and the uplift of the middle hilltop (see Figure 7c). The case when two target attribute values are different is shown in Figure 8 and the overall process is similar. However, as Figure 8b,c show, the merged mountain bodies always tilt to high-value points.

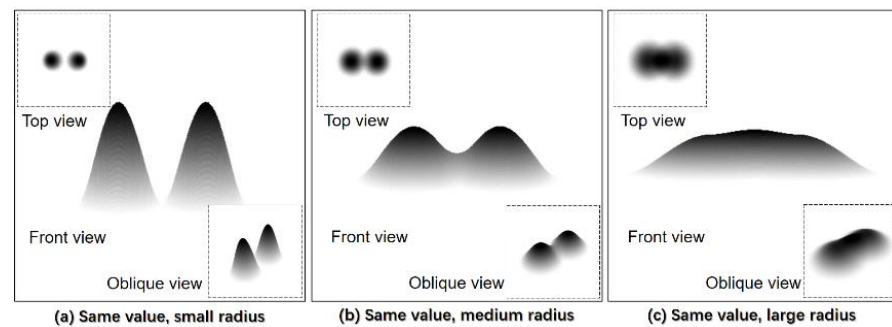


Figure 7. Terrain created by two points with the same target attribute value and different search radii.

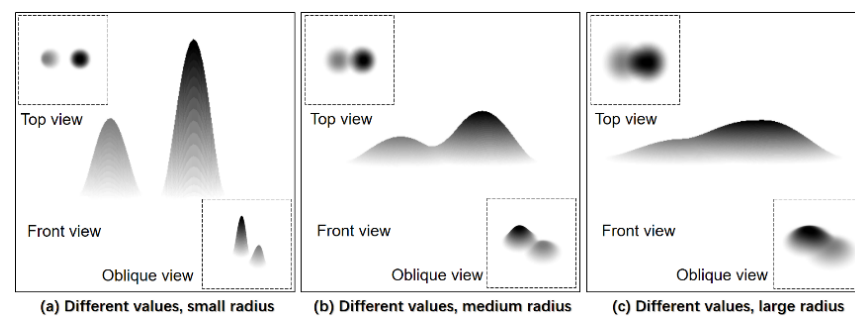


Figure 8. Terrain created by two points with different target attribute values and different search radii.

As the search radius in kernel density estimation increases, the mountain bodies undergo severe changes. These changes increase the connectivity between mountains and reflect the data relationship that becomes increasingly tight. The search radius in this study represents the scale of observation and analysis. There are different criteria for evaluating the relationship between data items at different scales. In general, the criteria on a macroscopic scale are relatively relaxed, and many data items are considered to have a relationship. In the corresponding terrain expression, the mountains are connected together by the saddle and gain a large extension range. Otherwise, the criteria on a microscopic scale are more rigorous. The number of data items with relationships is small, and the extent of the mountains that are connected by the saddles is relatively small in the corresponding terrain.

The interpolation results and terrains at different scales constructed from different search radii using sample discrete point data are shown in Figures 9 and 10. When the search radius is large, it includes more spatial objects for the calculation and obtains more general interpolation results. For instance, Figure 9a,b shows a mononuclear cluster, and the value decreases from the center to the periphery. The corresponding virtual terrains are usually presented as large mountains with simple structures and do not have complex rises or falls (see Figure 10a,b).

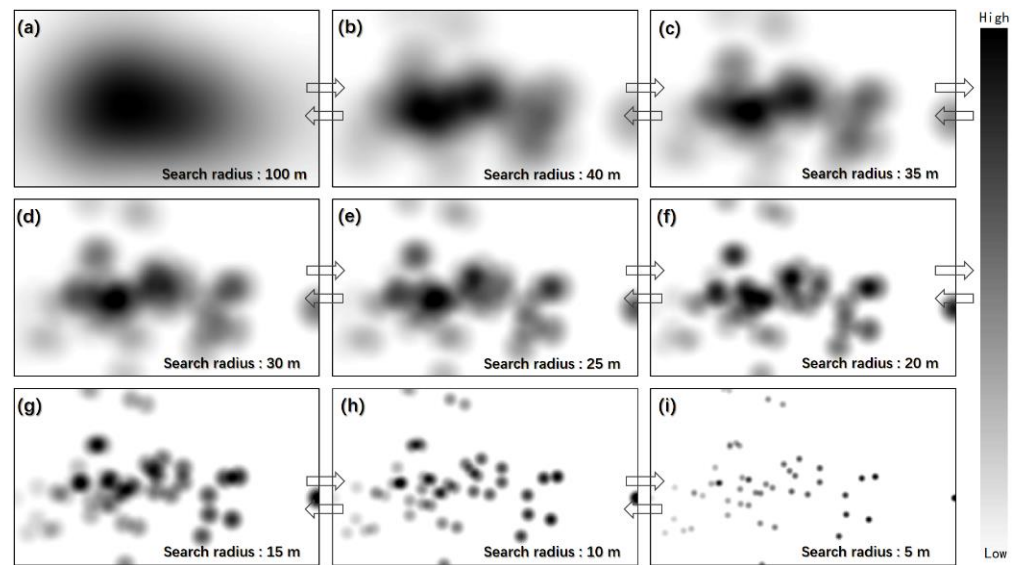


Figure 9. Interpolation results of different search radii.

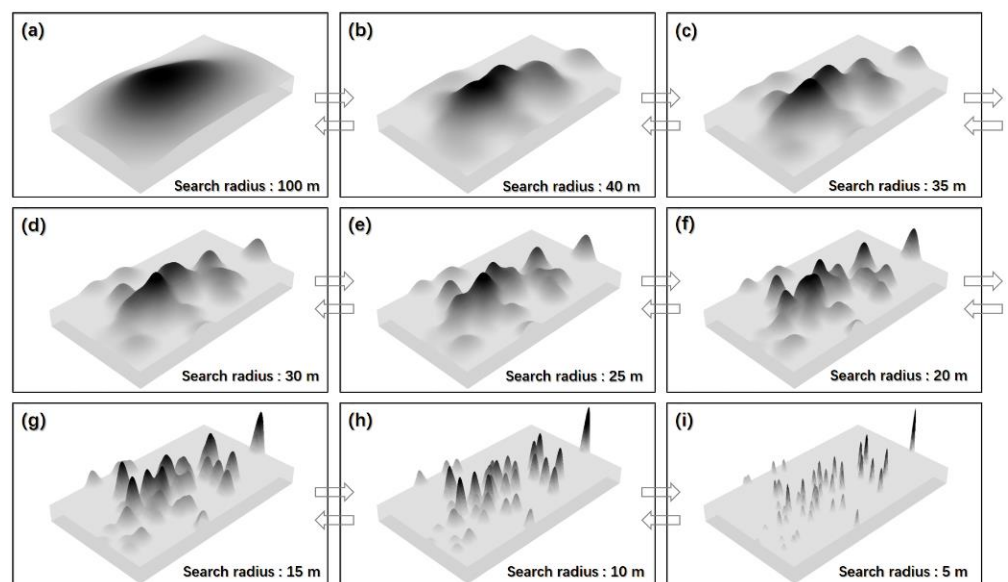


Figure 10. Three-dimensional results of different search radii.

As the search radius decreases, the interpolation results change from coarse to fine. As shown in Figure 9c–f, the original mononuclear distribution gradually shrinks and splits and finally appears as a multinuclear distribution state. In this process, the connection between multiple cores gradually faded. The abovementioned nuclear fission process is iteratively generated in each single-core unit so that the entire interpolation result is continuously cracked and discretized. The terrain created based on this also changes accordingly. As shown in Figure 10c–f, the terrain starts to show more rises and falls, gradually forming differentiated mountains, and then these mountains disintegrate, many independent mountains appear. In this process, terrain features such as peaks, valleys, saddles and cliffs are constantly shaped.

When the search radius becomes very small, as shown in Figure 9g–i, every unit in the interpolation result is highly separated, and many white spaces appear. In the terrains in Figure 10g–i, the aggregated mountains disappear, and a large number of independent peaks and cliffs appear. In addition, a high proportion of plain areas also appear in the scene.

3.3. Detail Increase in Virtual Terrain

How to enhance the realism of map-like visualization works and increase the audience's recognition of their map identity is a key issue in this field [31,32]. The virtual terrain generated above is excessively smooth and monotonous which is not like the real terrain. In terrain simulation, realism is usually improved by adding details [33]. In this study, noise is added to the original terrain to increase the detail. It is difficult to simulate natural phenomena and objects with complex changes only by a single frequency noise. Fractal noise is proposed to solve this problem. The fractal noise can simulate self-similar objects in nature by sampling the fundamental noise at different frequencies and superimposing these sampling results [34]. In this study, fractal noise is constructed and added to the terrain framework to make the virtual terrain close to the shape of natural terrain. Compared with other virtual terrain construction methods that lack terrain details, this study aims to help users mobilize spatial thinking and promote information cognition by improving the realism of terrain scenes.

Perlin noise [35] is chosen in this study to create noise of different frequencies. Noise generation can be performed on the grid in which the location can be described by the row number and column number. The frequencies of the noise can be controlled by the sample step. The general steps are as follows:

1. Create a gradient field on the quadrilateral grid. As shown in Figure 11, the cell size in the gradient field is related to the sample step. The smaller the sample step is, the smaller the cell of the gradient field. Every node in the gradient field is a noise control point that is assigned a random gradient vector. As the red arrows in Figure 11 show, the length and direction of these arrows are randomly generated.

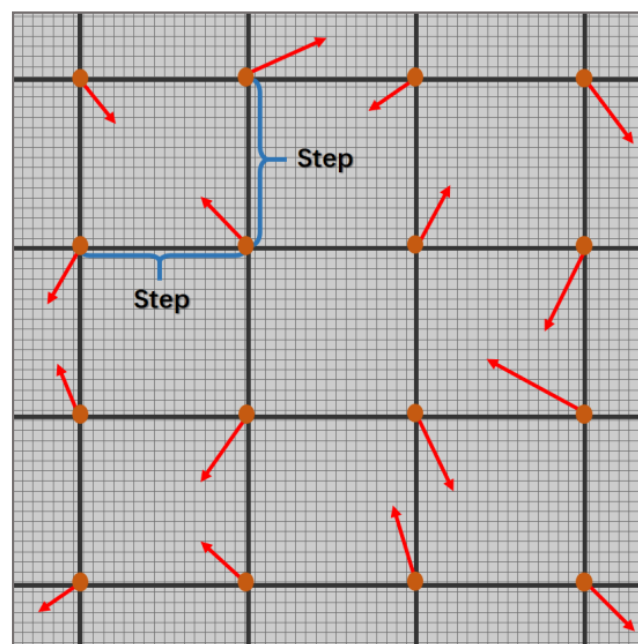


Figure 11. Gradient field based on sample steps.

2. As shown in Figure 12, the cell in which the noise point $Z(x,y)$ is located can be determined. Combined with Function (8), the locations of four noise-controlled points $K(x_i,y_j)$, $K(x_{i+1},y_j)$, $K(x_i,y_{j+1})$ and $K(x_{i+1},y_{j+1})$ of the cell can be calculated. Then, Function (9) is used to obtain the contribution of the four noise control points to noise point $Z(x, y)$ by calculating the dot product.

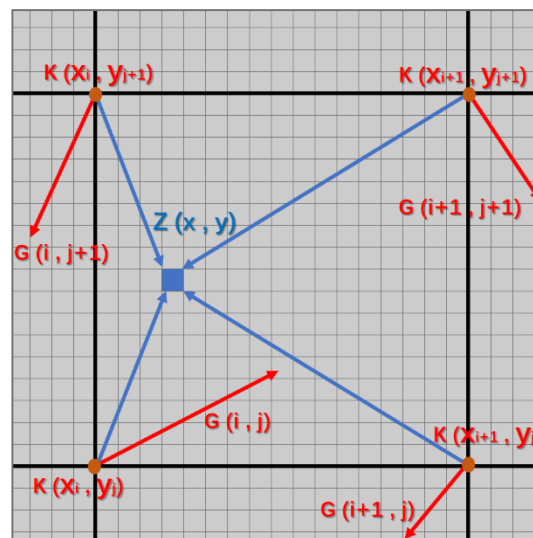


Figure 12. Illustration of noise calculation.

$$x_i = \lfloor x \div step \rfloor \times step$$

$$y_i = \lfloor y \div step \rfloor \times step$$

$$x_{i+1} = x_i + step$$

$$y_{i+1} = y_i + step$$

$$d_1 = (Z(x, y) - K(x_i, y_j)) \cdot G(i, j)$$

$$d_2 = (Z(x, y) - K(x_{i+1}, y_j)) \cdot G(i + 1, j)$$

$$d_3 = (Z(x, y) - K(x_{i+1}, y_{j+1})) \cdot G(i + 1, j + 1)$$

$$d_4 = (Z(x, y) - K(x_i, y_{j+1})) \cdot G(i, j + 1)$$

3. Interpolation calculation. Set the interpolation function as $f(x) = 6x^5 - 15x^4 + 10x^3$ [36]. As shown in Function (10), $x - x_i$ is substituted into function $f(x)$, and the interpolation operation is carried out in the x -axis direction; the results C_1 and C_2 can be obtained. Then, C_r can be calculated through Function (11) to carry out the interpolation operation in the y -axis direction. The noise result under a single sampling frequency and amplitude can be calculated using Function (12).

$$C_1 = d_1 - f(x - x_i) \times (d_1 - d_2) \tag{10}$$

$$C_2 = d_3 - f(x - x_i) \times (d_3 - d_4)$$

$$C_r = C_1 - f(y - y_i) \times (C_1 - C_2) \tag{11}$$

$$Perlin = C_r \times Amplitude \tag{12}$$

Different frequencies of noise can be achieved by adjusting the sample step. Figure 13 shows the multi-frequency noise results generated by the same amplitude and different sample steps on a grid of 100×100 . The noise results in Figure 13a,b have obvious plaques. If they are added directly to the terrain in this study, it will cause a large range of rises and falls on the terrain, which affects the expression of the original data characteristics. By

increasing the sampling frequency, it can be found that the high-frequency noise result can continuously dilute the plaque and make the noise distribution tend to be uniform.

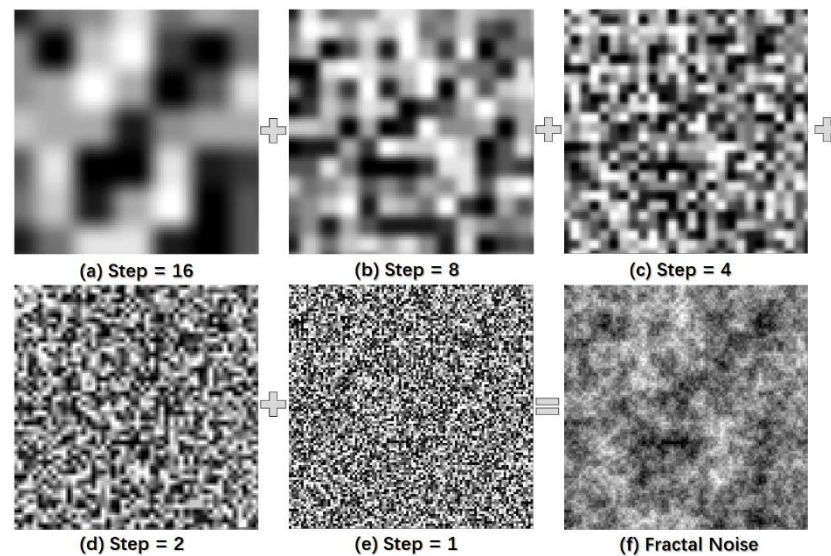


Figure 13. Illustration of fractal noise synthesis.

The mixed fractal noise result is calculated by Function (13), in which $Perlin_i$ is the i -th single-frequency, single-amplitude fundamental noise. $Perlin_i$ is arranged according to the sampling frequency from small to large, and $Weight_i$ is its corresponding weight value. To make the noise result form a low-frequency-noise building body, with the high-frequency noise depicting details, the noise amplitude is set as shown in Function (14). Persistence in Function 14 is introduced for noise amplitude reduction. Finally, weighted mixing of the noise data FractalNoise and the base terrain data BaseHeight is performed by Function (15) to obtain the final terrain data result Height and make the noisy terrain as shown in Figure 14. In Function (15), NR is the weight of noise in the final terrain result by which the noise proportion can be controlled.

$$FractalNoise = \frac{\sum_{i=0}^n Perlin_i \times Weight_i}{\sum_{i=0}^n Weight_i} \quad (13)$$

$$Amplitude_i = Persistence^i (0 < Persistence < 1) \quad (14)$$

$$Height = FractalNoise \times NR + BaseHeight \times (1 - NR) \quad (15)$$

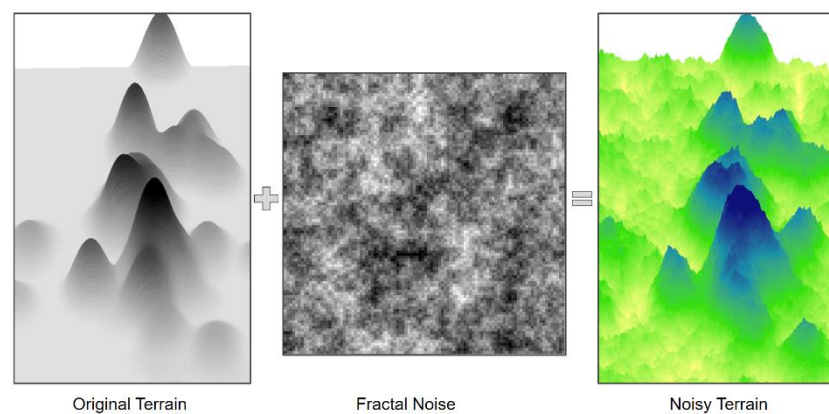


Figure 14. Construction of noisy terrain.

3.4. Multi-Scale Expression of Terrain

At the spatial scale, Li and Openshaw proposed the natural principle and provided a vivid example of observing the Earth's surface at different heights [37]: when Earth is viewed from a satellite, the surface appears very smooth. When the altitude decreases, more details will be found, such as when you look at the Earth from an aircraft. This principle can be well matched with people's actual life experience.

When carrying out the multi-scale expression of virtual terrain, this study learns from the natural principle and expresses the dynamic relationship between variables such as map scale, area range, search radius of kernel density estimation and proportion of noise. In view of the need for a macroscopic overview and the need for focusing on microscopic detail areas of interest, LOD technology was introduced. The correspondence between the LOD level, map scale and virtual terrain scene slices is established. For different expression requirements, the display of terrain scene slices can be controlled to reflect different levels of semantic information.

Figure 15 describes the process of expressing hierarchical data by different levels of terrain based on the LOD. With the method in Section 3.1 on the spatial layout of non-location data, the hierarchical spatial layout results in Figure 15(a1–a3) can be obtained. The virtual terrain skeletons in Figure 15(b1–b3) are constructed using the method in Section 3.2 on skeleton construction of a virtual terrain. For discrete points corresponding to each level, multiple search radii are used to perform kernel density estimation to construct virtual terrains on different scales. Moreover, the noise introduced in Section 3.3 on the detail increase in virtual terrain is used to add additional details to the terrain. The above terrain results in Figure 15(b4–b6) are inserted behind the previous terrain scenes Figure 15(b1,b2) to form a multilevel collection of terrain scenes.

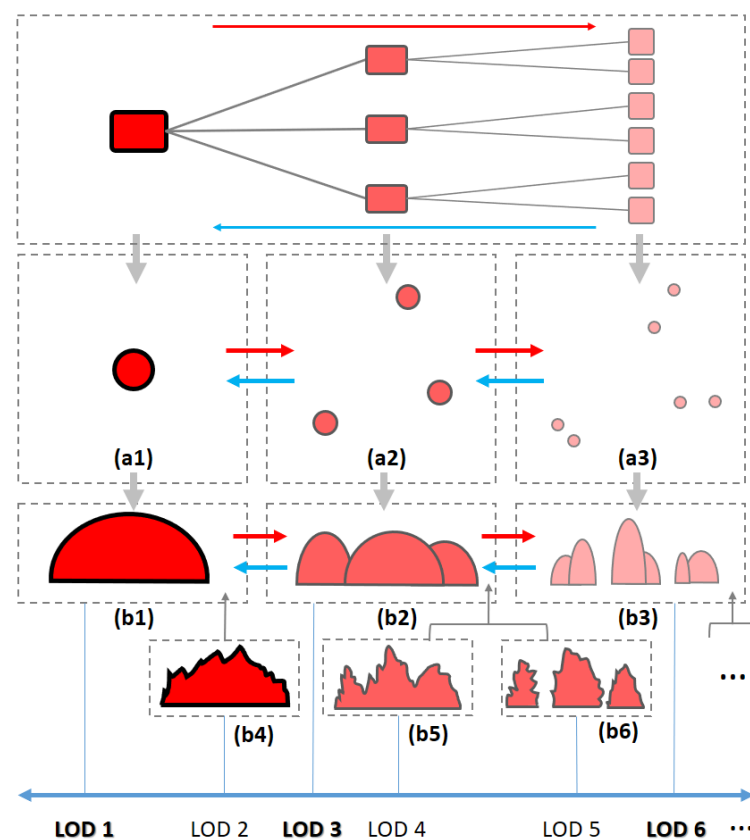


Figure 15. Expression of different levels of hierarchical data by different terrain (a1–a3): hierarchical spatial layout results; (b1–b6): virtual terrain construction results).

The terrain scene is given an LOD level according to the data level and detail rendering degree. For the low-detail terrain scene corresponding to the upstream node of the hierarchical data, a small LOD level is set. As the data level increases, the terrain scene has more detailed information, and a larger LOD level is set. In addition, key LOD levels such as LOD1, LOD3 and LOD6 in Figure 15 are set, corresponding to the virtual terrain scenes where the data level change occurs. The scene change between key LOD levels is a jump, which is essentially due to the difference in mapping data (that is, Figure 15(a1–a3)). Other LOD scenes within the key LOD level neighborhood exhibit a gradual state, such as LOD3 to LOD5. This shows the gradual appearance of detail and the division of the mountain due to an increase in the proportion of noise and a decrease in the search radius of the kernel density estimation.

Figure 16 shows the dynamic relationship between the map scale, map range and map scene at different LOD levels. The map on a small map scale simulates the situation of a high viewpoint. At this time, the map display range is large, and a virtual terrain scene with a low LOD level is output. In this terrain, the radius of kernel density estimation interpolation is large, and the noise addition ratio is small. Its terrain structure and shape are very simple, which is suitable for a macro-overview of the data but lacks details. The map that can be scaled fits well with the classic visual information exploration mode (the overview first, followed by the enlargement of the region of interest to obtain the detailed information) [38]. The area of interest is enlarged, and the map scale becomes larger, which simulates the low viewpoint. A high-level terrain scene with additional details and a shrunken map range is output by hiding the previous terrain scene. This terrain is made by a smaller radius of kernel density estimation interpolation and a larger noise addition ratio. More details about data features and relationships can be displayed in this terrain.

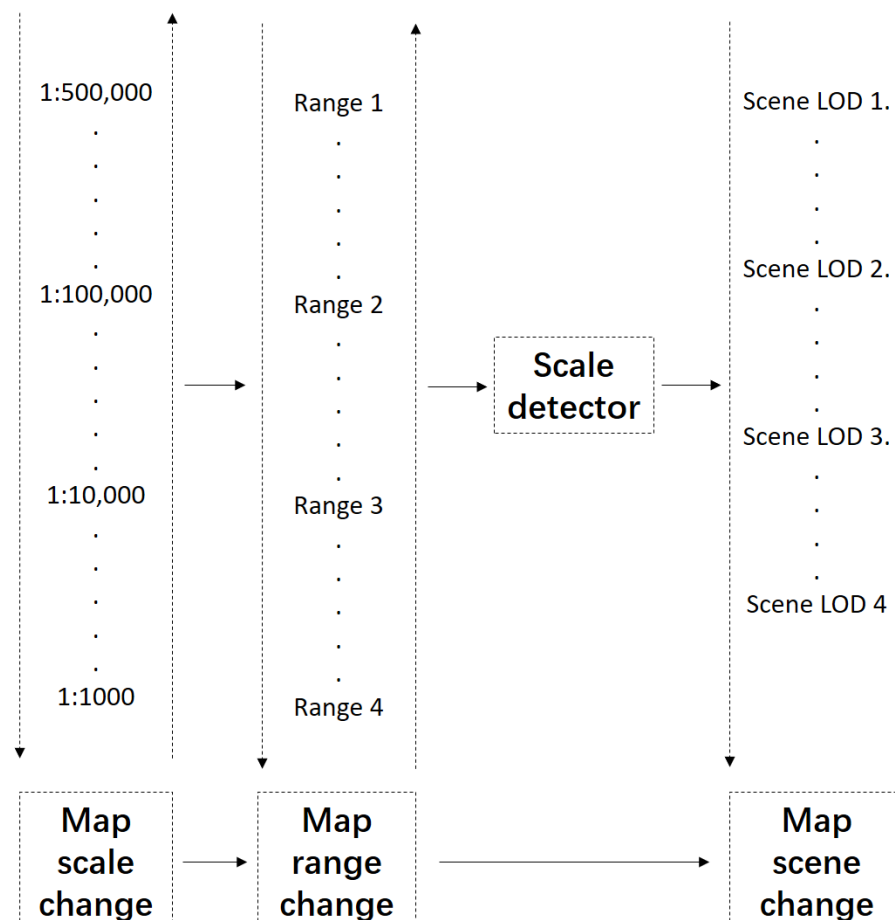


Figure 16. Dynamic relationship between the map scale, map range and map scene.

4. Experiment

The data selected in this experiment are obtained from the National Natural Science Foundation of China in 2016 and consist of typical hierarchical data. These data include three levels: National Natural Science Foundation, department and discipline. In addition, there are attributes of multiple dimensions, such as the number of approved projects, the approved funding amount, the average individual funding amount and the funding rate.

4.1. Virtual Terrain Construction

When carrying out spatial layout through MDS, a matrix of distances (or similarities) between data items is required as input. To avoid the influence of different dimensions on the results when calculating the similarity between data items, we first normalize the attribute values using Function (16) and map them to the range [0,1]. In Function (16), D_{nori} is the original data of the n th dimension, and D_{nmax} and D_{nmin} are the maximum and minimum values of these dimensional data, respectively.

$$D_n = \frac{D_{nori} - D_{nmin}}{D_{nmax} - D_{nmin}} \quad (16)$$

For the data that have been normalized, the similarity between each pair of data items is calculated by Function (17). The smaller the value is, the stronger the similarity. In Function (17), $D_n(i)$ is the attribute value of the i th data item in the n th dimension, and $weight_n$ is the weight of this dimension attribute. Through the weight coefficient $weight_n$, the influence of different attributes in the similarity calculation results can be controlled. This study does not discuss the difference in similarity contribution between these dimensions. Therefore, the weight coefficients of all dimensions are set to 1.

$$Sim(i,j) = \sum_{n=1}^k weight_n \times (D_n(i) - D_n(j))^2 \quad (17)$$

The similarity calculation for the department-level data is presented in Table 2. As shown in Figure 17, through the method introduced in Section 3.1 on the spatial layout of non-location data, the hierarchical spatial layout of the experimental data can be obtained.

Kernel density estimation and fractal noise are used to carry out the construction of multi-scale virtual terrain. The approved funding amount is chosen as the target attribute to carry out interpolation.

Table 2. Similarity calculation results between departments.

	Department of Math	Department of Chemistry	Department of Life	Department of Earth	Department of Engineering and Materials	Department of Information	Department of Management	Department of Medicine
Department of Math	0	0.18843	1.00275	0.22672	2.50536	0.83256	2.27632	4.97041
Department of Chemistry	0.18843	0	0.57462	0.06786	1.54479	0.32551	1.69266	3.86974
Department of Life	1.00275	0.57462	0	0.73374	0.42224	0.34131	2.39835	1.54794
Department of Earth	0.22672	0.06786	0.73374	0	1.79486	0.62269	2.36449	4.24204
Department of Engineering and Materials	2.50536	1.54479	0.42224	1.79486	0	0.74752	2.73764	0.66414
Department of Information	0.83256	0.32551	0.34131	0.62269	0.74752	0	0.98531	2.51205
Department of Management	2.27632	1.69266	2.39835	2.36449	2.73764	0.98531	0	5.21155
Department of Medicine	4.97041	3.86974	1.54794	4.24204	0.66414	2.51205	5.21155	0

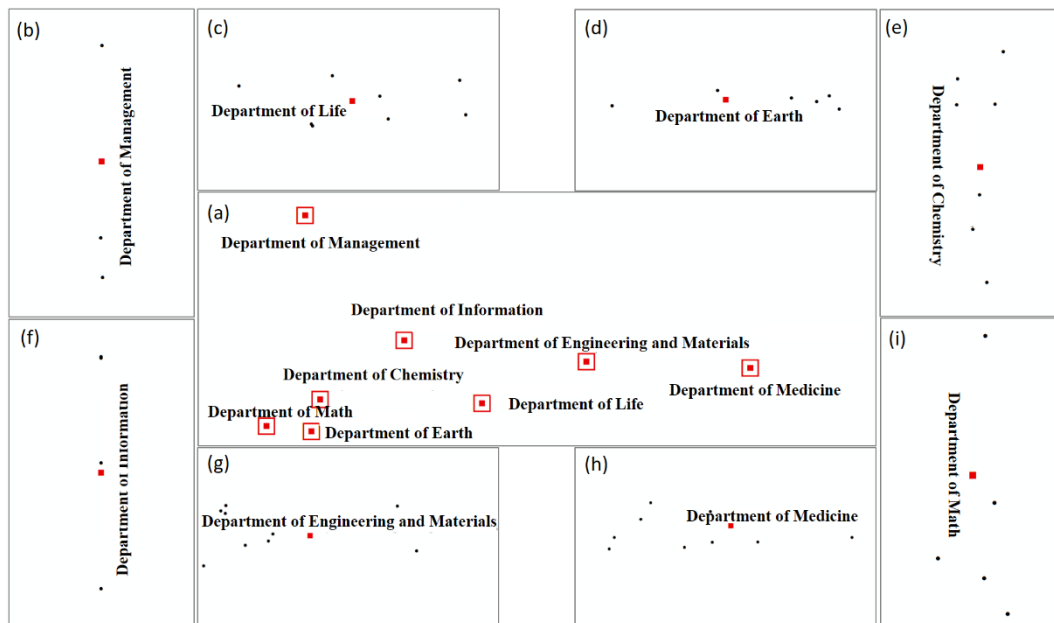


Figure 17. Hierarchical spatial layout of the experimental data.

4.2. Multi-Scale Expression and Analysis of Virtual Terrain

The presentation of a single level, a single scene and a single perspective does not fully represent the data characteristics and cannot readily reflect the changes in the data. As shown in Figure 18, the interactive nature of maps allows users to view the same data from different directions. In addition, the multi-scale character of the map can allow the display of differently scaled data in the same screen area. The change in scale can be achieved by interactive operation.

Using the natural principle for reference, a multi-scale representation scheme of virtual terrain is established to simulate the changes in human viewpoints from far to near and from high to low. As shown in Figure 19 group (a), a small-scale map is used to simulate the situation where the viewpoint is high. At this time, a sleek mountain is used to represent the 2016 National Natural Science Foundation (see Figure 19(a1)). The map range is very wide, and the map scene is general. By magnifying the map, the user can obtain some details on the terrain. However, as shown in Figure 19(a3), the whole scene is still presented as a complete mountain. As the map magnification intensifies, several hilltops appear, which indicates that the data have transitioned to the next level (see Figure 19(b1)).

As shown in Figure 19(b1–b3), the decreases in the search radius and increases in the noise lead to a gradual division of the mountain body and an increase in the detail degree. In this process, the differentiated hilltops become increasingly obvious, and the data of the departments become descriptive objects. Each mountain represents an independent department or a collection of multiple departments. The location relationship can accurately reflect the similarity. For instance, the distance between the Department of Medicine and the Department of Earth is quite far, and they are located at the ends of the map scene, which indicates that there are great differences between these two departments.

The mountain bodies that are near each other form a large aggregate mountain, which vividly reflects the strong similarity between the data items they represent. The abovementioned mountain aggregation phenomenon often appears in coarse scenes when the viewpoint and scene are far away. One example is the mountain aggregation formed by the Department of Engineering and Materials and the Department of Life in Figure 19(b2). At this time, the detailed relationship between data items is blurred and displays the general relationship. As the observation point moves closer, the terrain in the scene changes accordingly. For instance, the aggregation mountain formed by the Department of Engineering and Materials and the Department of Life in Figure 19(b2) gradually transitions

to a differentiated mountain in which two mountain bodies are connected by a low saddle, as shown in Figure 19(b3). However, the aggregation mountain formed by the Department of Earth, the Department of Math and the Department of Chemistry still maintains a certain integrity, and differentiation is not obvious. This indicates that those three departments have a stronger relationship of similarity than that between the Department of Engineering and Materials and the Department of Life. Thus, the relative strength of relationships within departments can also be reflected by the changes in the aggregated mountains.

In the above process, the differentiation of the mountain is still the main body of terrain changes. Only departments, such as the Department of Medicine, that have obvious differences from others in terms of comprehensive attributes are separated and form relatively independent mountains. With the further shortening of the observation distance, the splitting of the mountain body becomes the main feature of terrain change. The mountains of departments gradually separate from the aggregated mountains and form independent mountains. The aggregated mountain that has not yet been differentiated in the above process is taken as the observation object (see the black circle in Figure 19(b4)). As shown in Figure 19(b4–b6), the map is continually magnified until the aggregated mountain also exhibits a similar process of mountain differentiation to the point of complete division. Finally, we focus on the independent Department of Earth and magnify the map to prepare for a new round of discipline-level terrain exploration.

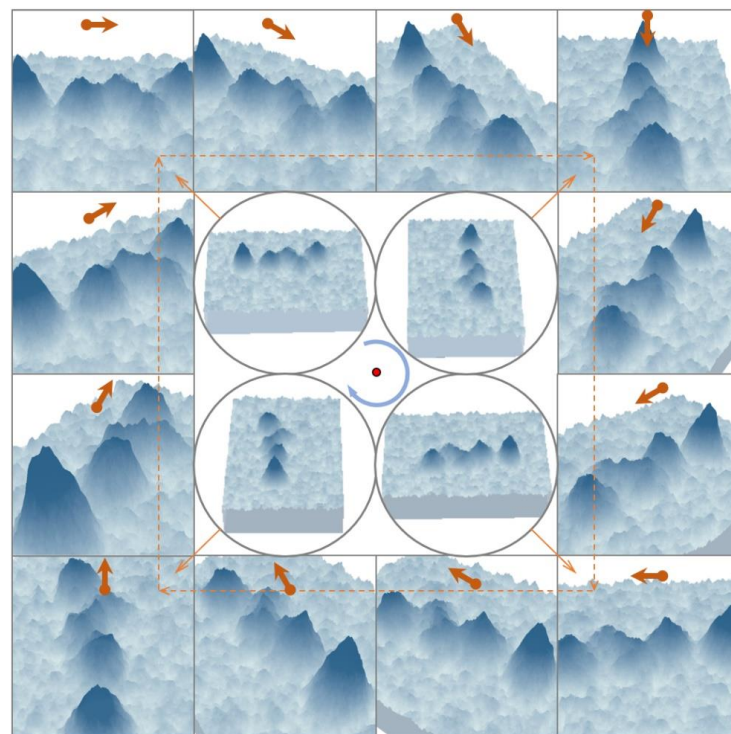


Figure 18. The same terrain from different directions.

Figure 19 group (c) shows the terrain change at the discipline level, which describes the mountain detailing and differentiation process as the observation distance becomes closer. In this process, the Geography Discipline is first separated into an independent mountain, highlighting its very large differences from other disciplines. Seen from this altitude, the above differences include a larger lead of the Geography Discipline in the approved funding amount. As the viewpoint decreases, the mountain of the Geology Discipline is gradually separated and forms independent mountains, as shown in Figure 19(c3). The above process has gradually shaped the scenes of three independent mountains of the Geography Discipline, Geology Discipline and other disciplines, such as the Marine Discipline. In terms of the attribute value, the mountains of the Geography Discipline

and Geology Discipline exhibit a high value in approved funding amount. In particular, the approved funding amount of Geography can even compete with the total value of multiple disciplines that include the Marine Discipline. The above process can be repeated continually to learn more about each discipline. Moreover, the process can also be reversed to observe the map from a large map scale to a small map scale, which corresponds to bottom-up changes in hierarchical data.

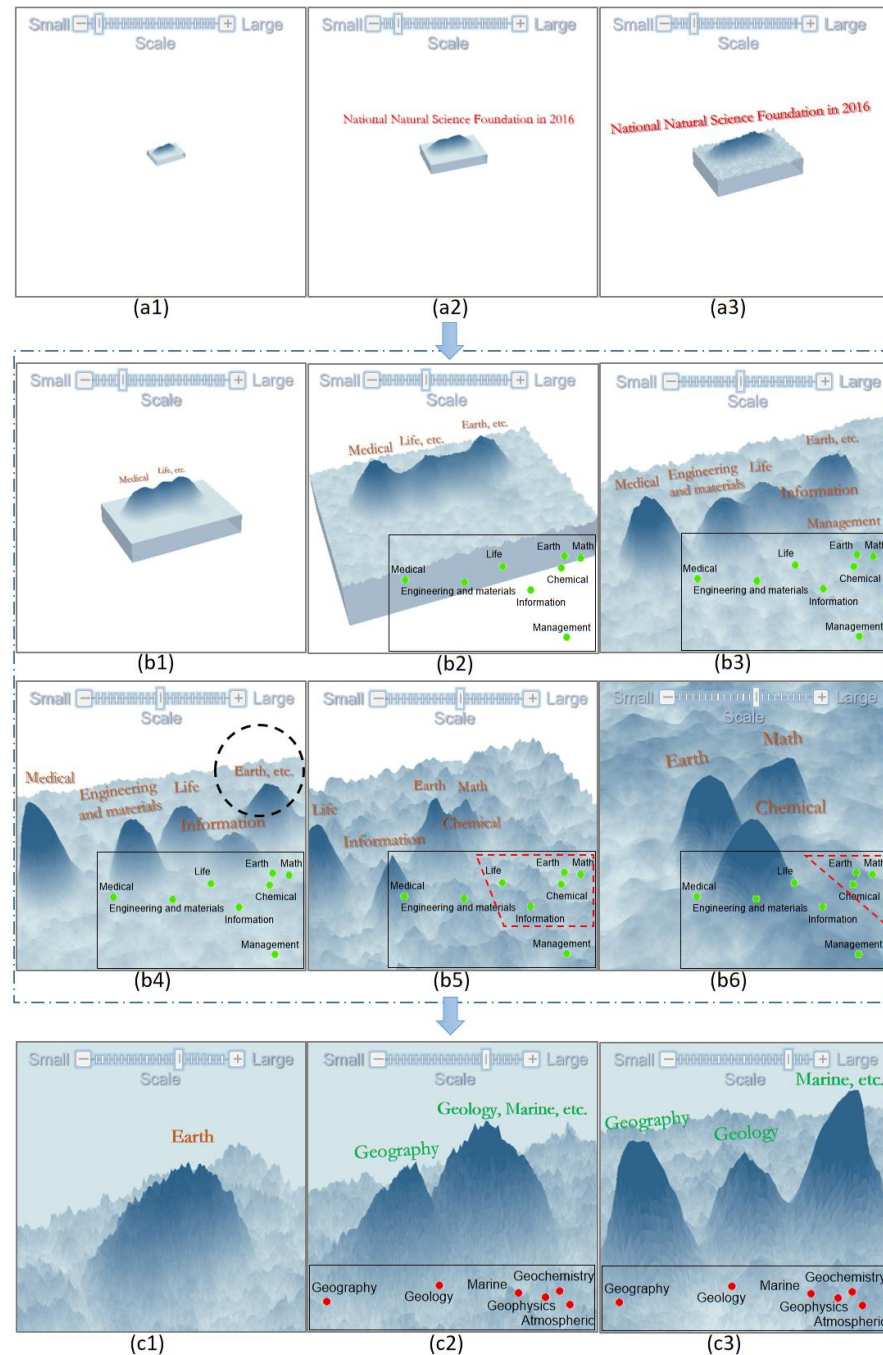


Figure 19. Multi-scale terrain reflecting hierarchical data: Group (a) First-level terrains; Group (b) Second-level terrains; Group (c) Terrains from the second level to the third level. Construction parameters: (a1) Radius 20 m Noise 0%; (a2) Radius 20 m Noise 10%; (a3) Radius 20 m Noise 30%; (b1) Radius 16 m Noise 0%; (b2) Radius 12 m Noise 10%; (b3) Radius 8 m Noise 20%; (b4) Radius 6 m Noise 20%; (b5) Radius 4m Noise 30%; (b6) Radius 2 m Noise 30%; (c1) Radius 1.5 m Noise 40%; (c2) Radius 1 m Noise 40%; (c3) Radius 0.5 m Noise 40%.

5. Conclusions

In the era of big data, with the emergence of massive data, there are a large number of non-spatial data with non-location features, a high degree of abstraction and weak perceptibility. Many of them have hidden structures that further hinder people's cognition. Using a spatial metaphor, a virtual terrain is constructed in this study to visualize the multi-scale structure and relationships of hierarchical data. The spatial metaphor provides a new tool for the expression of abstract data and a new perspective for its analysis. It promotes the understanding of non-spatial problems with the help of human spatial thinking and is of great significance in using the overview intuition of maps to explore the abstract characteristics of big data to infer complex phenomena in non-spatial fields.

This study confirms the feasibility of multi-scale representation of hierarchical data using virtual terrain, and the main contributions are as follows: 1. This study provides a set of feasible schemes for virtual terrain construction to support the visualization and analysis of the hierarchical structure and similarity relationships of data. The scope of expression and application of virtual terrain is expanded. 2. Many classical methods, such as kernel density estimation interpolation and fractal noise, are introduced into the construction of multi-scale virtual terrain through adaptive transformation. The terrain expression of different details is realized through the control of parameters such as the search radius of kernel density estimation and the proportion of noise. 3. A multi-scale terrain model is established, allowing the analysis of non-location data through spatial multi-scale browsing. Through the application of natural principles in scale modelling, a variety of spatial variables are grouped to show abstract data more vividly and comprehensively.

However, there are still many shortcomings in the current study. For instance, the height of the mountain can currently only represent one attribute. In terms of parameter settings, due to the large difference in data, this study does not give a quantitative description about how scale changes, the radius of kernel density estimation, noise proportion, etc., are related; instead, it relies only on empirical values after the coarse data analysis. All of these aspects necessitate further research in the future. In addition, with the continuous development and integration of technologies, virtual simulation space can be created by combining technologies such as virtual reality and non-spatial data can be mapped to simulate natural objects in this virtual space. Exploring large-scale non-spatial data through immersive visualization and various new interactive technologies will provide more realistic scenes and a richer experience for data observation and research.

Supplementary Materials: The source code of this research is available at <https://github.com/letter91/multi-scale-virtual-terrain.git> (accessed on 3 June 2021).

Author Contributions: Conceptualization, Rui Xin and Tinghua Ai; methodology, Rui Xin; project administration, Bo Ai; software, Ruoxin Zhu and Min Yang; supervision, Tinghua Ai and Liqiu Meng; writing—original draft, Rui Xin; writing—review and editing, Ruoxin Zhu and Liqiu Meng. All authors have read and agreed to the published version of the manuscript.

Funding: This research was funded by the National Natural Science Foundation of China, grant number 62071279.

Acknowledgments: The support provided by the China Scholarship Council (CSC) during the Ph.D. study of “Rui Xin” in Technical University of Munich is acknowledged. We are grateful to the editor and anonymous reviewers for their constructive feedback, which provided inspiration for our research.

Conflicts of Interest: The authors declare no conflict of interest.

References

1. Skupin, A.; Fabrikant, S.I. Spatialization. In *The Handbook of Geographical Information Science*; Blackwell Publishers: Malden, MA, USA, 2007; pp. 61–79.
2. Skupin, A. A cartographic approach to visualizing conference abstracts. *IEEE Comput. Graph. Appl.* **2002**, *22*, 50–58. [[CrossRef](#)]
3. Ai, T.; Xin, R.; Yan, X.; Yang, M.; Ai, B. Shape Decision-Making in Map-Like Visualization Design Using the Simulated Annealing Algorithm. *IEEE Access* **2019**, *7*, 131577–131592. [[CrossRef](#)]

4. Gansner, E.R.; Hu, Y.; Kobourov, S.G. GMap: Drawing graphs as maps. In Proceedings of the 17th International Conference on Graph Drawing, Chicago, IL, USA, 22–25 September 2009; Springer: Berlin/Heidelberg, Germany, 2009.
5. Fabrikant, S.I.; Montello, D.R.; Mark, D.M. The natural landscape metaphor in information visualization: The role of commonsense geomorphology. *J. Am. Soc. Inf. Sci. Technol.* **2010**, *61*, 253–270. [[CrossRef](#)]
6. Lakoff, G.; Johnson, M. *Metaphors We Live by*; University of Chicago Press: Chicago, IL, USA, 2008.
7. Fabrikant, S.I. Evaluating the Usability of the Scale Metaphor for Querying Semantic Space. In Proceedings of the International Conference on Spatial Information Theory, Morro Bay, CA, USA, 19–23 September 2001; Springer: Berlin/Heidelberg, Germany, 2001; pp. 156–172.
8. Cecconi, A.; Weibel, R.; Barrault, M. Improving automated generalisation for on-demand web mapping by multiscale databases. In *Advances in Spatial Data Handling*; Springer: Berlin/Heidelberg, Germany, 2002; pp. 515–531.
9. Skupin, A.; Buttenfield, B.P. Spatial Metaphore for Visualizing Information Spaces. In Proceedings of the ACSM/ASPRS Annual Convention and Exhibition, Seattle, WA, USA, 12–19 October 1997.
10. Montello, D.R.; Fabrikant, S.I.; Ruocco, M.; Middleton, R.S. Testing the first law of cognitive geography on point-display spatializations. In Proceedings of the International Conference on Spatial Information Theory, Ittingen, Switzerland, 24–28 September 2003; Springer: Berlin/Heidelberg, Germany, 2003; pp. 316–331.
11. Fabrikant, S.I.; Montello, D.R.; Ruocco, M.; Middleton, R.S. The distance–similarity metaphor in network-display spatializations. *Cartogr. Geogr. Inf. Sci.* **2004**, *31*, 237–252. [[CrossRef](#)]
12. Fabrikant, S.I.; Monteilo, D.R.; Mark, D.M. The distance-similarity metaphor in region-display spatializations. *IEEE Comput. Graph. Appl.* **2006**, *26*, 34–44. [[CrossRef](#)] [[PubMed](#)]
13. Tobler, W.R. A computer movie simulating urban growth in the Detroit region. *Econ. Geogr.* **1970**, *46*, 234–240. [[CrossRef](#)]
14. Fabrikant, S.I.; Montello, D.R. The effect of instructions on distance and similarity judgements in information spatializations. *Int. J. Geogr. Inf. Sci.* **2008**, *22*, 463–478. [[CrossRef](#)]
15. Hogräfer, M.; Heitzler, M.; Schulz, H.J. The State of the Art in Map-Like Visualization. *Comput. Graph. Forum* **2020**, *39*, 647–674. [[CrossRef](#)]
16. Chen, S.; Li, S.; Chen, S.; Yuan, X. R-Map: A map metaphor for visualizing information reposting process in social media. *IEEE Trans. Vis. Comput. Graph.* **2019**, *26*, 1204–1214. [[CrossRef](#)]
17. Chen, S.; Chen, S.; Lin, L.; Yuan, X.; Liang, J.; Zhang, X. E-map: A visual analytics approach for exploring significant event evolutions in social media. In Proceedings of the 2017 IEEE Conference on Visual Analytics Science and Technology (VAST), Phoenix, AZ, USA, 3–6 October 2017; pp. 36–47.
18. Chen, S.; Chen, S.; Andrienko, N.; Andrienko, G.; Nguyen, P.H.; Turkay, C.; Thonnard, O.; Yuan, X. User behavior map: Visual exploration for cyber security session data. In Proceedings of the 2018 IEEE Symposium on Visualization for Cyber Security (VizSec), Berlin, Germany, 22 October 2018; pp. 1–4.
19. Wood, J.D.; Fisher, P.F.; Dykes, J.A.; Unwin, D.J.; Stynes, K. The use of the landscape metaphor in understanding population data. *Environ. Plan. B Plan. Des.* **1999**, *26*, 281–295. [[CrossRef](#)]
20. Yu, W.; Ai, T.; Shao, S. The analysis and delimitation of Central Business District using network kernel density estimation. *J. Transp. Geogr.* **2015**, *45*, 32–47. [[CrossRef](#)]
21. Chalmers, M. Using a landscape metaphor to represent a corpus of documents. In Proceedings of the European Conference on Spatial Information Theory, Elba Island, Italy, 19–22 September 1993; Springer: Berlin/Heidelberg, Germany, 1993; pp. 377–390.
22. Wise, J.A.; Thomas, J.J.; Pennock, K.; Lantrip, D.; Pottier, M.; Schur, A.; Crow, V. Visualizing the non-visual: Spatial analysis and interaction with information from text documents. In Proceedings of the Visualization 1995 Conference, Atlanta, GA, USA, 30–31 October 1995; pp. 51–58.
23. Wise, J.A. The ecological approach to text visualization. *J. Am. Soc. Inf. Sci.* **1999**, *50*, 1224–1233. [[CrossRef](#)]
24. Boyack, K.W.; Wylie, B.N.; Davidson, G.S. Domain visualization using VxInsight® for science and technology management. *J. Am. Soc. Inf. Sci. Technol.* **2002**, *53*, 764–774. [[CrossRef](#)]
25. Xin, R.; Ai, T.; Ai, B. Metaphor Representation and Analysis of Non-Spatial Data in Map-Like Visualizations. *ISPRS Int. J. Geo-Inf.* **2018**, *7*, 225. [[CrossRef](#)]
26. Van Liere, R.; De Leeuw, W. GraphSplatting: Visualizing graphs as continuous fields. *IEEE Trans. Vis. Comput. Graph.* **2003**, *9*, 206–212. [[CrossRef](#)]
27. Gronemann, M.; Jünger, M. Drawing clustered graphs as topographic maps. In Proceedings of the International Symposium on Graph Drawing, Redmond, WA, USA, 19–21 September 2012; Springer: Berlin/Heidelberg, Germany, 2012; pp. 426–438.
28. Skupin, A. From Metaphor to Method: Cartographic Perspectives on Information Visualization. In Proceedings of the IEEE Symposium on Information Visualization 2000, INFOVIS 2000. Proceedings, Salt Lake City, UT, USA, 9–10 October 2000; pp. 91–97.
29. Skupin, A.; Fabrikant, S.I. Spatialization methods: A cartographic research agenda for non-geographic information visualization. *Cartogr. Geogr. Inf. Sci.* **2003**, *30*, 99–119. [[CrossRef](#)]
30. Parzen, E. On estimation of a probability density function and mode. *Ann. Math. Stat.* **1962**, *33*, 1065–1076. [[CrossRef](#)]
31. Pang, P.C.-I.; Biuk-Aghai, R.P.; Yang, M. What makes you think this is a map? Suggestions for creating map-like visualisations. In Proceedings of the 9th International Symposium on Visual Information Communication and Interaction, Dallas, TX, USA, 24–26 September 2016; pp. 75–82.

32. Pang, P.C.-I.; Biuk-Aghai, R.P.; Yang, M.; Pang, B. Creating realistic map-like visualisations: Results from user studies. *J. Vis. Lang. Comput.* **2017**, *43*, 60–70. [[CrossRef](#)]
33. Ripolles, O.; Ramos, F.; Puig-Centelles, A.; Chover, M. Real-time tessellation of terrain on graphics hardware. *Comput. Geosci.* **2012**, *41*, 147–155. [[CrossRef](#)]
34. Smelik, R.M.; De Kraker, K.J.; Tutenel, T.; Bidarra, R.; Groenewegen, S.A. A survey of procedural methods for terrain modelling. In Proceedings of the CASA Workshop on 3D Advanced Media in Gaming and Simulation, Amsterdam, The Netherlands, 16 June 2009; pp. 25–34.
35. Perlin, K. An image synthesizer. *ACM Siggraph Comput. Graph.* **1985**, *19*, 287–296. [[CrossRef](#)]
36. Perlin, K. Improving noise. *ACM Trans. Graph.* **2002**, *21*, 681–682. [[CrossRef](#)]
37. Li, Z.; Openshaw, S. A natural principle for objective generalization of digital map data. *Cartogr. Geogr. Inf. Syst.* **1993**, *20*, 19–29.
38. Shneiderman, B. The Eyes Have It: A Task by Data Type Taxonomy for Information Visualization. In Proceedings of the 1996 IEEE Symposium on Visual Languages, Boulder, CO, USA, 3–6 September 1996.